

Journal of Mechanics of Materials and Structures

**A PHASE-FIELD MODEL OF QUASISTATIC AND DYNAMIC
BRITTLE FRACTURE USING A STAGGERED ALGORITHM**

Hamdi Hentati, Marwa Dhahri and Fakhreddine Dammak

Volume 11, No. 3

May 2016



A PHASE-FIELD MODEL OF QUASISTATIC AND DYNAMIC BRITTLE FRACTURE USING A STAGGERED ALGORITHM

HAMDI HENTATI, MARWA DHAHRI AND FAKHREDDINE DAMMAK

Fracture mechanisms in solids are governed by complex fracture phenomena such as crack initiation and multiple crack branching. Recently, the numerical modeling of dynamic fracture mechanisms has been based on the introduction of a crack phase field. Following our recent works on phase-field modeling of quasistatic brittle fracture, a numerical method is presented to investigate the dynamic failure mechanisms in brittle solids using the phase-field model and a staggered algorithm. For that, numerical experiments of a brittle piece under tensile loading are performed. Based on these numerical results, the importance of developing a numerical method to optimize the computation time is shown. The optimized method is presented in a linear (P1) finite elements case in elasticity. We then show the results of using the optimized method in the case of dynamic fracture mechanics in brittle materials, and we analyze when the dynamic solution converges to the quasistatic one. We also investigate the influence of the numerical parameters h (mesh size) and η (regularization parameter) on the evolution of energies, displacements and crack location. The influence of exerted loading δ and transverse wave speed C_T is also elaborated.

1. Introduction

Numerical and experimental studies of failure mechanisms under mechanical, thermal, quasistatic and dynamic loads have been investigated in [Kim and Paulino 2004; Bourdin et al. 2008; Jiang et al. 2012]. In these contexts, several phase-field approaches to brittle fracture have been elaborated. The developments related to the theory of brittle fracture are mainly based on the idea presented by Griffith [1921]. Despite his important contribution to this theory, it has some shortcomings as detailed in [Bourdin 1998; Francfort and Marigo 2002]. Recently, fracture mechanics have been revised by proposing different phase-field models for quasistatic brittle fracture cases, taking inspiration from Griffith's criterion. Significant contributions to the phase-field methods were made by Miehe et al. [2010a; 2010b], in the form of a thermodynamically consistent framework for brittle mode I fractures in the case of viscous material response. A staggered scheme was employed by Miehe et al. [2010a], in which a local energy history field was introduced as a state variable to ensure irreversible crack growth. Also, a variational theory was developed by Francfort and Marigo [1998], and was used to model brittle fracture in [Bourdin et al. 2000; 2008; Oleaga 2004; Amor et al. 2009; Pham and Marigo 2010a; 2010b; Buliga 1998; Hentati et al. 2015]. They proposed a new formulation for the brittle fracture problem, capable of predicting the creation of new cracks, their path and their interactions in two and three spacial dimensions. The functional proposed during the segmentation of images from Ambrosio and Tortorelli [1990; 1992] was

Keywords: brittle fracture, staggered algorithm, phase field.

adapted to the problem of brittle fracture by Bourdin [2000]. In the same context, a higher order phase-field model formulation adopting Bourdin's formalism was recently created by Borden et al. [2014], in order to gain more regular and faster converging solutions to the variational problem of brittle fracture.

Ambati et al. [2015] analyzed the efficiency of different numerical methods for phase-field modeling of brittle fracture and presented an overview of the existing quasistatic and dynamic phase-field fracture formulations.

Otherwise, the study of the fracture problem has been usually made in the quasistatic case [Bourdin et al. 2008; Amor et al. 2009; Pham and Marigo 2010a; Hentati et al. 2012a; 2012b; Msekh et al. 2015]. However, it was found that this simplification hypothesis is not valid in many cases, as shown in [Dumouchel et al. 2007; Kalthoff 2000]. There have been several attempts to adapt phase-field models to dynamic fracture problems [Bourdin et al. 2011; 2012; Hofacker and Miehe 2012; 2013; Hentati 2013; Schlüter et al. 2014].

Numerical procedures currently used for time integration in the analysis of dynamic problems are the central difference method, the Newmark [1959] scheme, the Houbolt [1950] method and the Bathe and Wilson [1972] method. Bert and Stricklin [1988] described and compared several different integration methods used to analyze dynamic responses for linear and nonlinear systems. They showed that the error increases as the time step increases in all of the above methods and concluded that the Houbolt and Bath and Wilson methods are the least efficient, and that the Newmark scheme gives very similar results compared to theoretical ones.

Due to the nonconvexity of the regularized energy functional, a robust solution scheme based on (staggered) algorithmic decoupling was used in [Bourdin et al. 2008; Miehe et al. 2010a; Hentati et al. 2012a]. Based on a monolithic scheme used in [Miehe et al. 2010b; Borden et al. 2012; Vignollet et al. 2014], a coupled method was proposed in order to compute the quasistatic fracture phase field. The robustness of the staggered algorithmic implementation was proven by Ambati et al. [2015].

In order to resolve the dynamic fracture problem, Borden et al. [2012] proposed another method by introducing an initial strain history field that induces a phase field at the initial crack location. The numerical solution of the dynamic problem requires spatial and temporal discretization. The spatial discretization was formulated by the Galerkin method and the monolithic time integration scheme is based on the generalized- α method introduced by Chung and Hulbert [1993].

Bourdin et al. [2011] also proposed a discrete time model for dynamic fracture. They approached the elastic dynamic problem by using a finite difference discretization on the partial differential equation. They deduced that the total energy is not conserved. Hentati et al. [2013] used the Newmark direct integration method to study the evolution of energies by supposing an elasticity problem. The quantitative agreement between numerical results using the finite element method with the Newmark scheme and the analytical ones using the characteristic method was shown. Furthermore, the efficiency of the numerical method using the finite element method with the Newmark scheme for simulating dynamic crack propagation in brittle materials was shown.

This paper is focused on modeling and computing the dynamic crack propagation using the phase-field model. This model was developed by Francfort and Marigo [1998] for the quasistatic brittle fracture problem. The first goal is to propose and test an optimized numerical method in order to simulate dynamic crack propagation. This finite element assembly code is without loops and also without any quadrature formula. It is entirely vectorized. This method, which is based on the staggered scheme

with the optimized algorithm, is validated. Quasistatic tests are elaborated and the numerical results are compared with the experimentation done in [Ambati et al. 2015] and are also validated with the numerical results obtained in [Ambati et al. 2015; Msekhi et al. 2015]. The second goal is to analyze the computational results of dynamic crack propagation based on the numerical method detailed by Hentati et al. [2013]. The influence of numerical parameters (notably the ratio h/η) on energies and displacement evolution and crack location was also developed in this work.

2. Phase-field model of dynamic brittle fracture

A material is assumed to be elastic, isotropic and homogeneous with shear modulus μ and constant mass density ρ . The numerical model used for the antiplane case with constant toughness G_c is described below.

2A. Phase-field model. We introduce a discrete time model for dynamic brittle fracture which obeys the following principles:

- Elastic dynamic: away from the crack, the governing principle is the elastic dynamic equation. So, the dynamic problem consists in finding the displacement $u(x_1, x_2, t)$ satisfying

$$\rho \frac{\partial^2 u}{\partial t^2} = \mu \left(\frac{\partial^2 u}{\partial x_1^2} + \frac{\partial^2 u}{\partial x_2^2} \right). \quad (2-1)$$

- Energy balance: the evolution should satisfy an energy balance formula, similar to that found in the quasistatic setting, but now including kinetic energy.
- Maximal dissipation: if the crack can propagate while balancing energy, then it should propagate. Then, α minimizes the regularized energy $E(u, \alpha)$, given by

$$E(u, \alpha) = \frac{\mu}{2} \int ((1 - \alpha)^2 + \epsilon(\eta)) \nabla u \cdot \nabla u \, dx + G_c \int \left(\frac{\alpha^2}{4\eta} + \eta \nabla \alpha \cdot \nabla \alpha \right) dx. \quad (2-2)$$

The time-discrete algorithm for dynamic fracture that was developed can be summarized as follows:

Staggered dynamic fracture algorithm.

- Choose numerical and material parameters.
- Find u using the Newmark direct integration algorithm for linear systems (Figure 1).
- Find α such that the regularized energy $E(u, \alpha)$ given by (2-2) is minimized with respect to the irreversibility condition $\alpha(\delta) \geq \alpha(\delta - d\delta)$.

Here u is the displacement, $x(x_1, x_2)$ is the spatial coordinate, η is a regularized numerical parameter, α is the damage variable and ϵ is a positive infinitesimal whose role is to render coercive the regularized functional. We choose the parameters $\beta = 0.25$, which ensures stability, and $\gamma = 0.5$, which ensures both stability and accuracy of the Newmark algorithm. Both problems will be computed iteratively by using the staggered solution scheme.

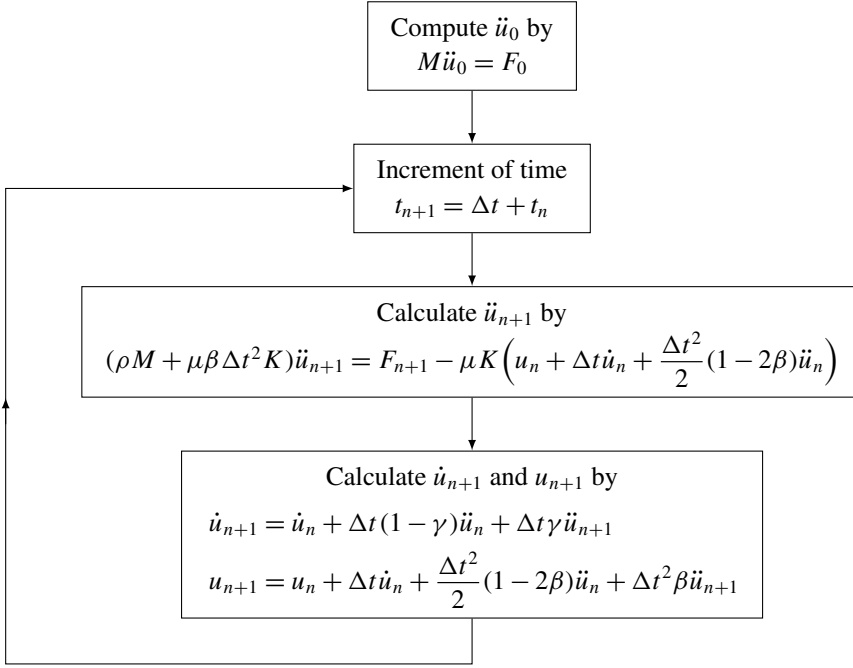


Figure 1. Direct Newmark integration algorithm for linear systems.

The elastic, surface and kinetic energies are given by

$$E_{\text{elast}}(t) = \frac{\mu}{2} \int_{\Omega} ((\alpha - 1)^2 + \epsilon) |\nabla u|^2 dx_1 dx_2, \quad (2-3)$$

$$E_{\text{surf}}(t) = G_c \int_{\Omega} \left(\frac{\alpha^2}{4\eta} + \eta |\nabla \alpha|^2 \right) dx_1 dx_2, \quad (2-4)$$

$$E_{\text{kine}}(t) = \frac{\rho}{2} \int_{\Omega} \left(\frac{\partial u(x_1, x_2, t)}{\partial t} \right)^2 dx_1 dx_2. \quad (2-5)$$

We carry out some numerical computations in order to determine the evolution of these energies that depend on the time and the location of cracking.

2B. Problem description. A rectangular structure is considered, as shown in [Figure 2](#), occupying the studied domain $\Omega \subset \mathbb{R}^2$, $\Omega = (0, L) \times (0, l)$, where L and l are the length and width of our structure.

The structure is fixed at the left edge and submitted to tensile loading at the right edge. A time-dependent Dirichlet boundary condition $\delta(t)$ is applied to the right edge, given by

$$\delta(t) = Kt^2. \quad (2-6)$$



Figure 2. Studied brittle structure with boundary conditions.

The boundary and initial conditions are

$$u(0, x_2, t) = 0, \quad u(L, x_2, t) = \delta(t), \tag{2-7}$$

$$\frac{\partial u(x_1, 0, t)}{\partial n} = \frac{\partial u(x_1, l, t)}{\partial n} = 0, \tag{2-8}$$

$$u(x_1, x_2, 0) = 0, \quad \frac{\partial u}{\partial t}(x_1, x_2, 0) = 0, \tag{2-9}$$

$$\alpha(x_1, x_2, 0) = 0. \tag{2-10}$$

3. Validation of the optimized staggered algorithm

The regularization parameter η should be large enough as compared to the mesh size h ($\eta \gg h$). Moreover, we know that if the mesh is fine (h is small), the obtained solution using the finite element method will be accurate compared to the analytic one. Therefore, the choice of h is a compromise between the value of η and the capacity of the processor used to perform the calculation. However, if this condition is respected, the repetition of elements inserted in the matrices will be very expensive if the classical method is used. So, the optimized method will be used to simulate dynamic crack propagation, in order to improve the cost of the method.

In this section, we validate a new method of assembling matrices that is based on the sparse function. This method allows us to reduce the computation time and further refine the mesh. We remind the reader of the classical method. Recall that Ω_h is the triangular mesh of the studied domain $\Omega \subset \mathbb{R}^2$. The basis function φ_i satisfies $\{\varphi_i(q^j)\} = \delta_{i,j}$. Due to the support properties of P1 Lagrange basis functions, we have the classical algorithm. For each element, its element matrix is added to the global matrix. This operation is illustrated in [Figure 3](#) for the 2D scalar fields case.

This proposed optimized assembling method is a standard one, used to assemble sparse matrices using triplet lists. The idea is to create three global 2D arrays, I_g , J_g and K_g , that allow the storage of the element matrices as well as the position of their elements in the global matrix. To create these three arrays, we first define three local arrays obtained from a generic element matrix $E(T_k)$:

- K_k^e contains the elements of the matrix $E(T_k)$ stored columnwise.
- I_k^e contains the global row indices associated with the elements stored in K_k^e .
- J_k^e contains the global column indices associated with the elements stored in K_k^e .

The three local arrays I_k^e , J_k^e and K_k^e are stored in the k -th column of the global arrays I_g , J_g and K_g , respectively.

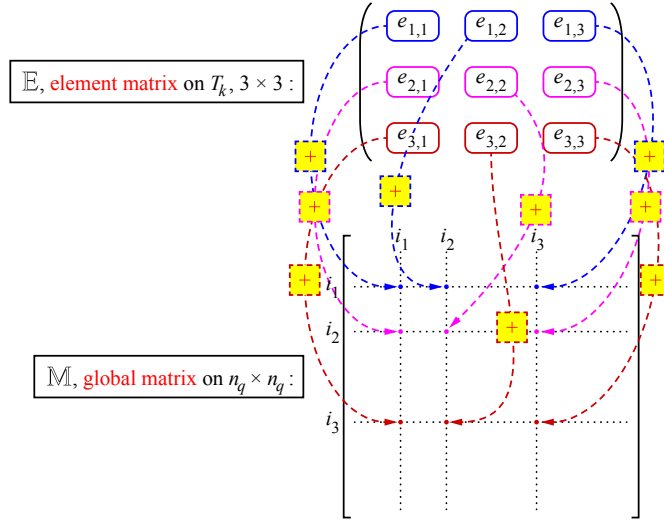


Figure 3. An element matrix added to the global matrix.

Function name	Calls per iteration	Total time of method (sec)	
		classical	optimized
Mass assembling matrix	4	20	4
Stiffness assembling matrix	12	120	14
Find α that minimizes $E(u, \alpha)$	1	2	$\ll 1$
Find u as solution of dynamic equation	1	7	$\simeq 1$
Principal program (after 120 iterations)	1	18500	2700

Table 1. Computational cost of minimizer problem.

A natural way to build these three arrays consists of using a loop through the triangles T_k , in which we insert the local arrays columnwise.

We compared the performance of these two programming techniques (optimized and classical methods) for assembling finite element matrices in 2D. Some numerical computations were done to investigate the time difference between the two methods. Table 1 shows the computational cost of the mass and stiffness matrix assembly. The results show that the optimized method gives better results than the classical one.

In order to validate this optimized staggered algorithm, numerical tests of some quasistatic fracture cases were done and the results were compared to experimental and validated numerical tension tests. These tests were computed using the staggered scheme with the optimized algorithm used for assembling matrices. A standard linear (P1) Lagrange finite element method was used to discretize the problem on the displacement field and the damage variable α . The problem consists in finding the displacement $u(x_1, x_2, t)$ that satisfies $\Delta u = 0$, using u to find α and using the couple (u, α) to minimize the regularized energy $E(u, \alpha)$. So, the staggered quasistatic fracture algorithm was developed and can be summarized as follows:



Figure 4. Experimental test of a notched plate with hole: (left) geometry and boundary conditions, (center) experiment result and (right) experimental setup. All units are in mm.

Staggered quasistatic fracture algorithm.

- Choose numerical and material parameters.
- Find u that minimizes the regularized energy $E(u, \alpha)$, as given by (2-2).
- Find α such that the regularized energy $E(u, \alpha)$ is minimized with respect to the irreversibility condition $\alpha(\delta) \geq \alpha(\delta - d\delta)$.

3A. First test: notched plate with hole. For the first test, a sample consisting of a notched plate with a hole is presented. Figure 4 illustrates the experimental test of a notched plate with a hole as detailed by Ambati et al. [2015]. The geometry, boundary conditions and experimental setup are shown in Figure 4. The specimen is a notched plate with a hole offset from the center. The top pin is submitted to displacement loading and the lower pin is fixed.

The crack path is illustrated in Figure 5. A curved crack develops from the notch to the large hole. Later, a secondary straight crack appears from the hole to the sample edge.

3B. Second test: single edge notched. We apply the phase-field model to a square plate containing a straight horizontal notch located at mid-height on the left edge with a length of 0.5 mm. The geometric properties and boundary conditions of the specimen are shown in Figure 6. A vertical displacement is applied to the top edge.

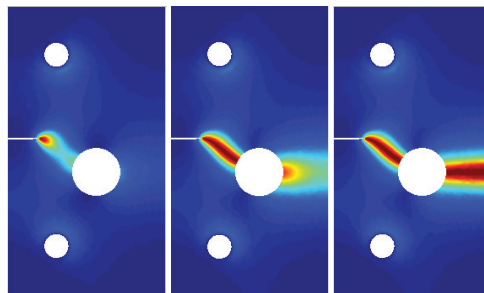


Figure 5. Notched plate with hole: quasistatic crack phase field.

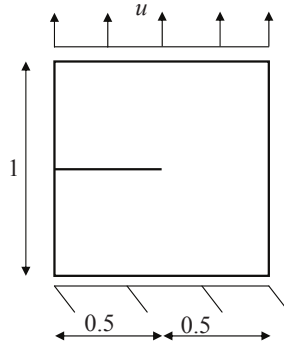


Figure 6. Geometry and boundary conditions for single edge notched specimen. All units are in mm.

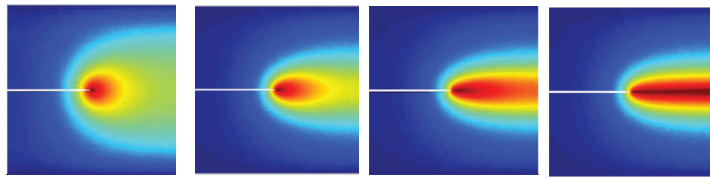


Figure 7. Single edge notched: quasistatic crack phase field.

Figure 7 shows the crack patterns at several stages of loading for the tested model. Here the red and blue colors indicate the damaged and undamaged material, respectively.

With this setup, the crack propagates towards the middle right edge of the specimen. The phase-field model using the optimized staggered algorithm yields very similar results, in terms of crack path, to [Ambati et al. 2015; Msekh et al. 2015].

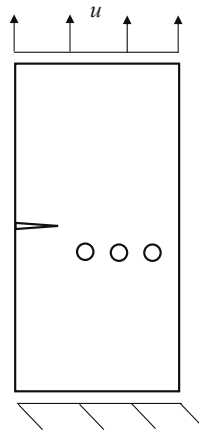


Figure 8. Notched rectangular specimen with three openings: geometry, loading and boundary conditions.

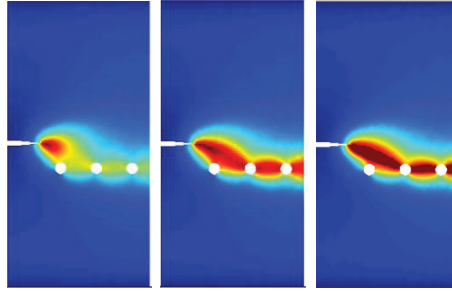


Figure 9. Notched rectangular specimen with three openings: quasistatic crack phase field.

3C. Third test: notched specimen with three openings. We simulate a sample consisting of a notched rectangular plate with three circular openings, in which the centers are aligned horizontally. The three circular openings are near the initial notch as shown in Figure 8. The applied loading and boundary conditions are also shown.

As shown in Figure 9, the presence of the opening nearest to the notch causes a kinking of the crack path just above it; however, the opening is not near enough to the notch line to arrest crack propagation. This occurs just above the second opening along with the initiation of a new crack segment, similar to what was observed in the first test. We compared the numerical result of this study with the numerical crack pattern from [Msekh et al. 2015], and the comparison shows that the present phase-field model is able to predict the correct trajectory of a curved crack. Msekh et al. studied the effect of varying the proximities of openings in altering the propagation of a crack path. They showed that for holes situated significantly far away from the notch line, crack propagation is virtually unaffected, whereas for sufficiently close openings the crack path is modified.

The current and preceding tests highlight an important strength of the phase-field method, specifically that the initiation of a crack does not require the introduction of a notch, and that a crack may initiate anywhere within the geometry of a given structure. So, we have shown that the phase-field model using the staggered scheme and the optimized algorithm of assembling matrices is in agreement with experimental and validated numerical results in terms of crack pattern. This numerical method is used in the next section for simulating dynamic crack propagation.

4. Numerical experiments of dynamic fracture mechanics

The following settings were chosen for all numerical computations. The material properties are $G_c = 1$, $\rho = 1$ and $\mu = 1$. The numerical parameter is $\epsilon = 10^{-5}$. The dimensions of the structure are $L = 2$ and $l = 1$. Table 2 shows the values of the selected parameters for the simulations.

A Dirichlet condition was applied on the right and left boundaries in the 1st test:

$$\alpha(x_1 = 0, x_2, t) = \alpha(x_1 = L, x_2, t) = 0. \quad (4-1)$$

In this section, the evolution of α and of different energies was studied while varying the exerted load. Also, the influence of numerical parameters on the critical load-causing fracture (δ_c), the evolution of energies and the location of crack was analyzed.

4A. Regularized damage field. Using the parameters from the 1st test, the coordinates of some nodes are shown in [Table 3](#).

First, we studied the evolution of the damage field at these nodes as a function of time. The applied load is $\delta(t) = t^2$. The evolution of α changing with respect to time is illustrated in [Figure 10](#). The nodes N01, N02, N03 and N04 have α greater than 0.7 while α reaches the value 1 in other nodes. Therefore, the fracture is not brutal because α does not reach the value 1 at the same time for all nodes in the cracked area.

We then investigated the evolution of the damage field in the cracked zone. The fracture occurs during the 1950th iteration ($t = 1.95$). During this time, few nodes have a damage value $\alpha = 1$. [Table 4](#) shows the evolution of α in nodes N05 ($x_1(\text{N05}) = 1.84$) and N06 ($x_1(\text{N06}) = 1.83$). For both nodes, the value of α is less than 1, but it increases slowly until its value reaches 1 after some iterations. In the same context, the damage field in quasistatic hypothesis is unregularized in time. It jumps suddenly to the

Test	η	h	Time step dt (sec)	Boundary conditions (BC) on α
1st test	0.02	0.007	0.001	with BC
2nd test	0.02	0.007	0.001	without BC
[Hentati 2013]	0.03	0.01	0.0025	without BC

Table 2. Numerical parameters in different simulation tests.

Nodes	N01	N02	N03	N04	N05	N06
x_1 coordinate	1.84	1.83	1.7	1.65	1.84	1.83
x_2 coordinate	0.5	0.5	0.5	0.5	0.2	0.7

Table 3. Node coordinates.

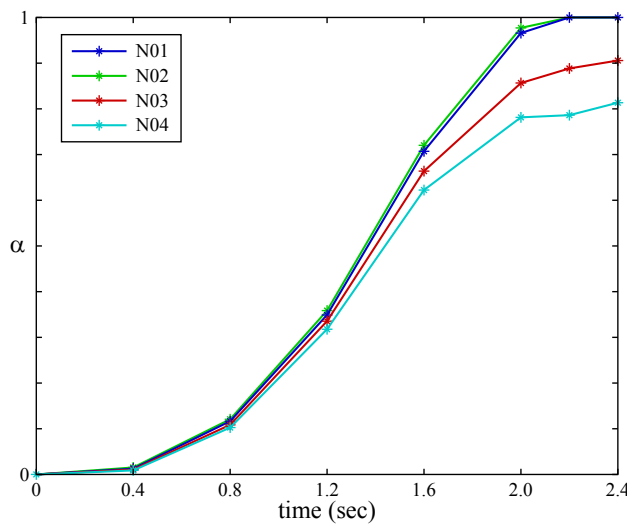


Figure 10. Evolution of α depending on time.

Time (sec)	α at N05	α at N06
1.60	0.69	0.70
1.80	0.80	0.80
1.85	0.84	0.83
1.90	0.85	0.84
1.92	0.85	0.84
1.95	0.86	0.85
1.97	0.86	0.85
1.98	0.87	0.86
2.00	0.88	0.86
2.30	0.97	0.93
2.50	1.00	0.98
2.60	1.00	1.00

Table 4. Evolution of α in different nodes.

value 1 and brutal cracking appears. But, in the dynamic crack propagation case, it is regularized in time and in space.

Next, the displacement before and after crack initiation in the 1st test case was studied. The displacement evolution at different times and their differences versus x_1 -coordinates are presented in Figures 11, 12 and 13. We show that, after crack initiation at $t = 1.95$, the displacement is nonzero and is increasing in time. This is due to the rigidity of the structure. Some nodes have a value of $\alpha = 1$ and other nodes in the cracked area have a value of α less than 1. After the crack initiation, the difference between the displacements become smaller in time. This is due to the increase in the number of nodes in which $\alpha = 1$.

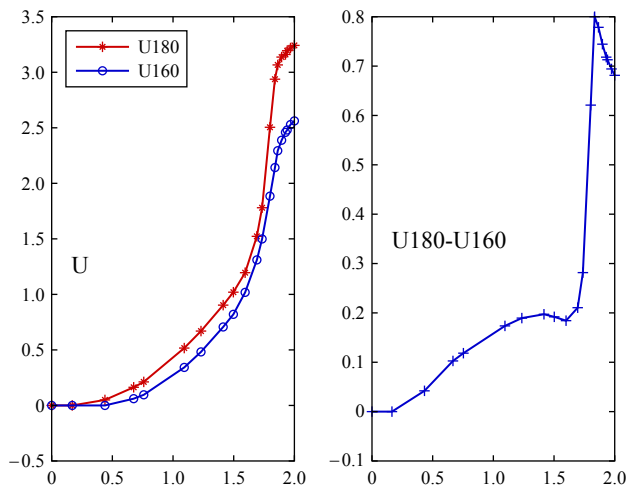


Figure 11. Left: displacement versus x_1 coordinate at $t = 1.60$ (U160) and at $t = 1.80$ (U180). Right: difference between U180 and U160.

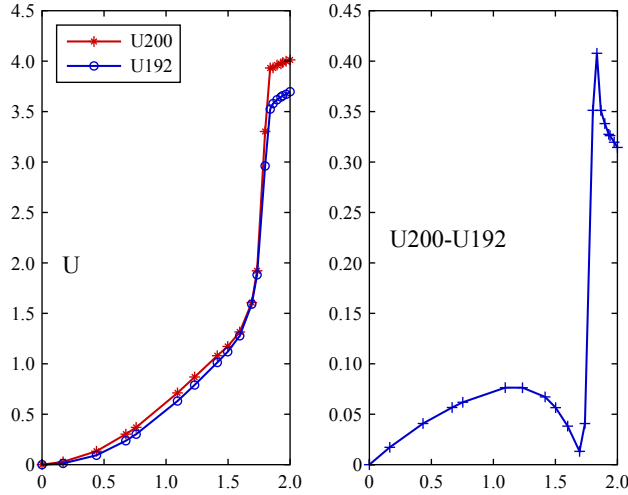


Figure 12. Left: displacement versus x_1 coordinate at $t = 1.92$ (U192) and at $t = 2.00$ (U200). Right: difference between U200 and U192.

4B. Evolution of computed energies. We refer the reader to the results found by Hentati et al. [2013]. For $t = t_c = 1.6$ ($\delta = \delta_c = 2.56$), the elastic energy E_{elast} reaches its maximum value and decreases. The kinetic energy E_{kine} reaches its minimum value ($dE_{\text{kine}}/dt = 0$) and then rises ($dE_{\text{kine}}/dt > 0$). At this time, crack propagation occurs. The surface and total energies become constant if $\delta > 2.56$, and the sum ($E_{\text{elast}} + E_{\text{kine}}$) is constant. Note that E_{surf} is nonzero before the critical load δ_c is reached. This is due to the insufficiently small value of the mesh parameter.

Figures 14 and 15 describe the evolution of computed energies versus time using the applied load $\delta(t) = t^2$.

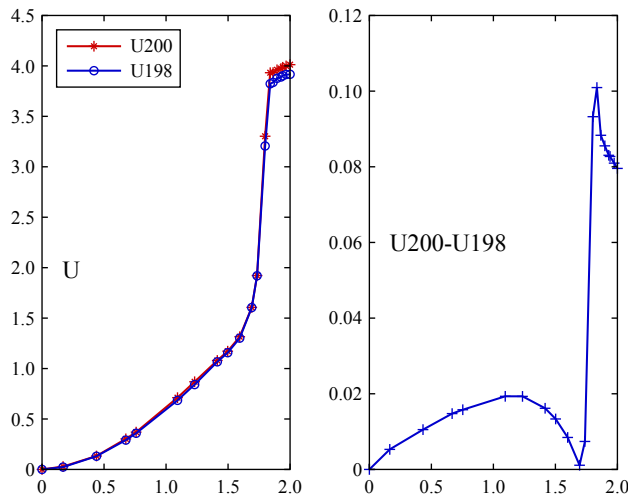


Figure 13. Left: displacement versus x_1 coordinate at $t = 1.98$ (U198) and at $t = 2.00$ (U200). Right: difference between U200 and U198.

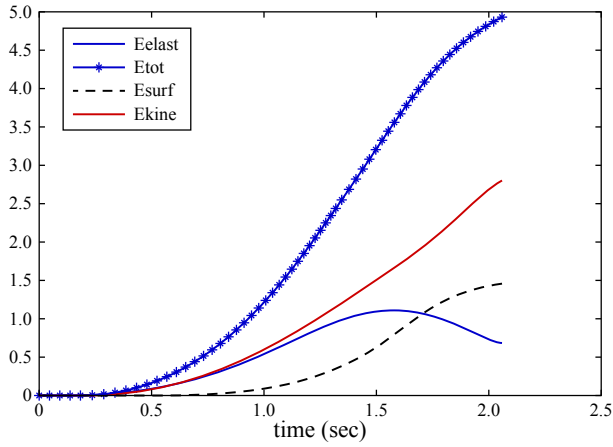


Figure 14. Evolution of computed energies in the 1st test.

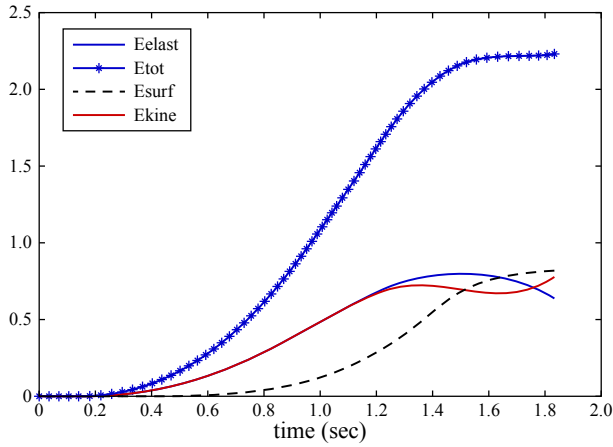


Figure 15. Evolution of computed energies in the 2nd test

In order to study the influence of numerical parameters and boundary conditions essentially on the energies' evolution as well as the critical time value, we illustrate in [Table 5](#) the main results.

Using the numerical results obtained by Hentati [\[2013\]](#), the surface energy E_{surf} becomes nonzero at $t = 0.62$. But, in the 2nd test ([Figure 15](#)), the surface energy E_{surf} becomes nonzero at $t = 0.65$. Then, if the regularized parameter η is small, E_{surf} will remain zero almost all of the time. However, after the

Test	η	h/η	t_c	E_{surf} at $t = t_c$
1st test	0.02	0.35	1.95	1.4
2nd test	0.02	0.35	1.65	0.8
[Hentati 2013]	0.03	0.33	1.6	0.75

Table 5. Main results in different tests.

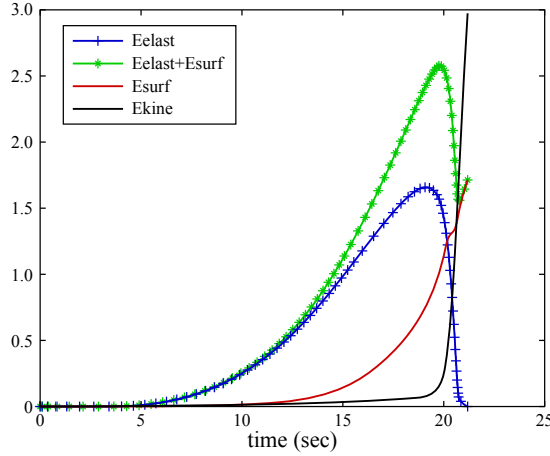


Figure 16. Influence of the applied load on the evolution of energies ($K = 0.01$).

initiation of crack (some nodes have a value of $\alpha = 1$), the value of the surface energy E_{surf} and the critical time lead to fracture t_c depending on the ratio h/η .

In fact, as shown in Table 5, the critical time t_c and the surface energy E_{surf} decrease when the ratio h/η decreases as revealed by the study of influence of numerical parameters and boundary conditions on the evolution of energies and the localization of crack. So, in the 1st test, the fracture will be at $t = t_c = 1.95$ (see Figure 14).

Although the ratio $h/\eta = 0.35$ is conserved, this critical time value t_c is not the same in the 2nd test (see Figure 15). Also, in the 1st test, the elastic energy E_{elast} reaches the maximum value and decreases before the fracture of structure. The kinetic energy E_{kine} increases in time ($dE_{kine} > 0$). At time $t = 1.65$,

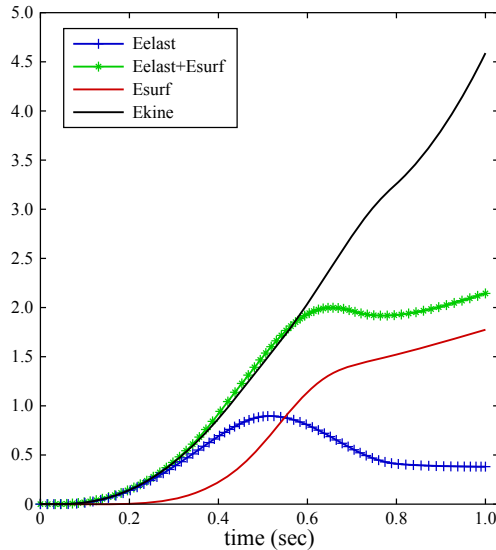


Figure 17. Influence of the applied load on the evolution of energies ($K = 5$).

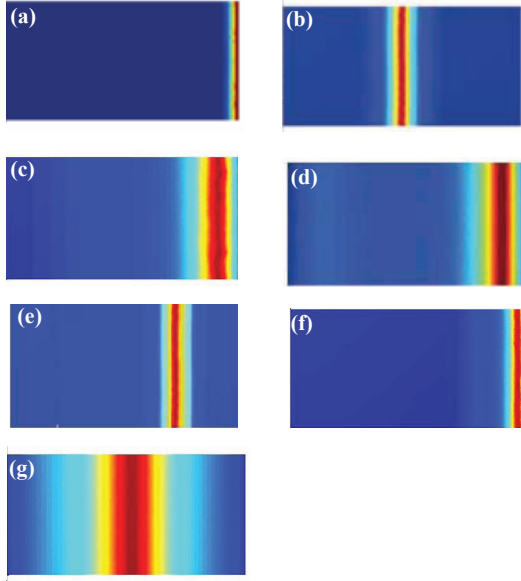


Figure 18. Location of cracks in quasistatic and dynamic fracture: (a) quasistatic fracture with Neumann boundary condition on α and $K = 1$ [Hentati 2013], (b) quasistatic fracture with Dirichlet boundary condition on α and $K = 1$ [Hentati et al. 2012a], (c) dynamic fracture in the 2nd test, (d) dynamic fracture in the 1st test, (e) dynamic fracture like the 1st test but with $C_T = 10$, (f) dynamic fracture like the 1st test but with $K = 5$ and (g) dynamic fracture like the 1st test but with $K = 0.01$.

$E_{\text{surf}} = E_{\text{elast}}$, the energy E_{surf} increases in time and E_{elast} decreases and if $t = 1.95$ a crack propagation occurs.

4C. Influence of applied load. In this section, the influence of the acceleration $a = \partial^2 \delta(t) / \partial t^2$ on the evolution of the crack is investigated. So, we impose the Dirichlet boundary condition on damage variable α on the right and left edges of our structure (1st test). Based on (2-6), the acceleration is $a = 2K$. Two coefficients of the applied load were chosen in the following tests: $K = 0.01$ and $K = 5$. Figures 16 and 17 represent the evolution of energies as a function of time t .

In conclusion, for $K \ll 1$, α passes rapidly from the value 0.7 to 1 in a few iterations. Rupture occurs for loading $\delta = 3.76$ (i.e., at $t = 19.4$). E_{elast} reaches its maximum and then decreases at the time of rupture. This energy vanishes after cracking. E_{surf} increases until reaching E_{elast} after the break and is then set to 1. When the coefficient K is high, the evolution of energies is similar to the case $K = 1$, but different than the case of $K \ll 1$.

5. Comparison between quasistatic and dynamic fracture

Figure 18 summarizes the location of cracks in quasistatic and dynamic fracture cases and their dependence on the transverse wave speed C_T , the acceleration $a = 2K$ and the boundary condition on α .

In the quasistatic computations, and as shown in [Hentati et al. 2012a; 2012b], the Dirichlet boundary condition applied on α does not have a significant influence on the propagation condition of a crack. However, it does have an influence on the location of a crack. The elastic energy E_{elast} decreases from its maximum value and the surface energy of the computed solution is overestimated ($E_{\text{surf}} > 1$) as compared to a theoretical value of $E_{\text{surf}}^{\text{th}} = G_c l = 1$. Figure 18(a)–(b) show the locations of cracks in the quasistatic case with and without boundary conditions on α , respectively. Also, in quasistatic computations, there can be an instant decrease in E_{elast} when α increases (i.e., the crack grows), at which point brutal cracking appears in the brittle rectangular domain. The critical load is overestimated ($\delta_c > \delta_c^{\text{th}} = 2$) as compared to the theoretical critical load, given by

$$\delta_c^{\text{th}} = \sqrt{\frac{2LG_c}{\mu}}. \quad (5-1)$$

In dynamic crack propagation, we show that after the initiation of a crack during the 1950th iteration ($t = 1.95$), the displacement is nonzero and increasing in time. This is due to the rigidity of the structure. Some nodes have a value of $\alpha = 1$ while other nodes in the cracked area have a value of $\alpha < 1$. After the initiation of the crack, the differences between the displacements becomes smaller over time. This is due to the increase in the number of nodes that have a value of $\alpha = 1$. So, the damage field in the quasistatic problem is nonregularized in time and space. It jumps suddenly to the value 1 and brutal cracking appears. But in the dynamic case, the crack propagation is progressive and the phase field is regularized in time and space. Equally important, the location of crack depends on the value of the transverse wave speed C_T , given by

$$C_T = \sqrt{\frac{\mu}{\rho}}. \quad (5-2)$$

Also, the coefficient K has an influence on the location and thickness of crack, the evolution of the damage field and the evolution of energy, but has no effect on the critical load δ_c .

Quasistatic computations were also done in [Hentati 2013]. It was shown that the Dirichlet boundary condition on α does not have an effect on the evolution of energies, but it does affect the crack location. Brutal cracking appears in the brittle solid and there can be an instant decrease in the elastic energy when the crack grows. In the dynamic fracture case, crack growth takes place if $dE_{\text{kine}}/dt = 0$ instead of $G = G_c$ as in quasistatic fracture case, and the propagation condition of the crack is $dE_{\text{kine}}/dt > 0$ instead of $G > G_c$, as in the quasistatic fracture case. This condition only occurs if the Dirichlet boundary conditions on α are not applied to different edges than where the displacement field was applied, whereas if we apply a Dirichlet condition on the right and left boundaries ($\alpha(x_1 = 0, x_2, t) = \alpha(x_1 = L, x_2, t) = 0$), the dynamic crack will grow after $E_{\text{surf}} > E_{\text{elast}}$ and $dE_{\text{kine}}/dt > 0$.

We present the main results of this comparative study between quasistatic and dynamic crack propagation in rectangular structures below:

- In dynamic problems, crack location depends on the load coefficient K and the transverse wave speed C_T . If the term $\rho \partial^2 u / \partial t^2$ is not negligible compared with the term $\partial^2 u / \partial x^2$, we should consider the problem to be dynamic and the existence of waves alters the location of crack (see Figure 18(e)–(f)).

- If the load coefficient $K \ll 1$, the dynamic solution will converge to the quasistatic one (see Figure 18(g)).
- Crack propagation is progressive in the dynamic fracture case and brutal in the quasistatic one.

6. Conclusion

Phase-field modeling of brittle fracture shows promise as a computational tool for use in fracture problems that have geometries with complex crack surface topologies. We improved the performance of quasistatic and dynamic phase-field models of fracture by using staggered implementation schemes. Using formulations stemming from Griffith's theory, we focused on the quasistatic model featuring tension tests in which we use the phase-field model. We found agreement in terms of crack pattern with experimental and numerical results from literature. We also examined the staggered algorithm's implementation on dynamic problems, due to the algorithm's proven robustness. For that, an optimized method was proposed in order to simulate dynamic crack propagation in order to reduce the computation time and refine the mesh. This method consists of assembling matrices based on the sparse function. Furthermore, dynamic fracture mechanics were studied and the influence of numerical parameters on evolution of energies and crack location was investigated.

Acknowledgement

Thanks are due to F. Cuvelier (Laboratoire Analyse, Géométrie et Applications, Université Paris 13) for his critical help in the first parts of this paper.

References

- [Ambati et al. 2015] M. Ambati, T. Gerasimov, and L. De Lorenzis, “A review on phase-field models of brittle fracture and a new fast hybrid formulation”, *Comput. Mech.* **55**:2 (2015), 383–405.
- [Ambrosio and Tortorelli 1990] L. Ambrosio and V. M. Tortorelli, “Approximation of functionals depending on jumps by elliptic functionals via Γ -convergence”, *Comm. Pure. Appl. Math.* **43**:8 (1990), 999–1036.
- [Ambrosio and Tortorelli 1992] L. Ambrosio and V. M. Tortorelli, “On the approximation of free discontinuity problems”, *Boll. Un. Mat. Ital. B (7)* **6**:1 (1992), 105–123.
- [Amor et al. 2009] H. Amor, J.-J. Marigo, and C. Maurini, “Regularized formulation of the variational brittle fracture with unilateral contact: numerical experiments”, *J. Mech. Phys. Solids* **57**:8 (2009), 1209–1229.
- [Bathe and Wilson 1972] K. J. Bathe and E. L. Wilson, “Stability and accuracy analysis of direct integration methods”, *Earthq. Eng. Struct. Dyn.* **1**:3 (1972), 283–291.
- [Bert and Stricklin 1988] C. W. Bert and J. D. Stricklin, “Comparative evaluation of six different numerical integration methods for nonlinear dynamic systems”, *J. Sound Vib.* **127**:2 (1988), 221–229.
- [Borden et al. 2012] M. J. Borden, C. V. Verhoosel, M. A. Scott, T. J. R. Hughes, and C. M. Landis, “A phase-field description of dynamic brittle fracture”, *Comput. Methods Appl. Mech. Eng.* **217–220** (2012), 77–95.
- [Borden et al. 2014] M. J. Borden, T. J. R. Hughes, C. M. Landis, and C. V. Verhoosel, “A higher-order phase-field model for brittle fracture: formulation and analysis within the isogeometric analysis framework”, *Comput. Methods Appl. Mech. Eng.* **273** (2014), 100–118.
- [Bourdin 1998] B. Bourdin, *Une méthode variationnelle en mécanique de la rupture, théorie et applications numériques*, thesis, Université Paris-Nord, 1998, Available at <https://www.math.lsu.edu/~bourdin/downloads/Bourdin-1998a.pdf>.
- [Bourdin et al. 2000] B. Bourdin, G. A. Francfort, and J.-J. Marigo, “Numerical experiments in revisited brittle fracture”, *J. Mech. Phys. Solids* **48**:4 (2000), 797–826.

- [Bourdin et al. 2008] B. Bourdin, G. A. Francfort, and J.-J. Marigo, “The variational approach to fracture”, *J. Elasticity* **91**:1-3 (2008), 5–148.
- [Bourdin et al. 2011] B. Bourdin, C. J. Larsen, and C. L. Richardson, “A time-discrete model for dynamic fracture based on crack regularization”, *Int. J. Fract.* **168**:2 (2011), 133–143.
- [Buliga 1998] M. Buliga, “Energy minimizing brittle crack propagation”, *J. Elasticity* **52**:3 (1998), 201–238.
- [Chung and Hulbert 1993] J. Chung and G. M. Hulbert, “A time integration algorithm for structural dynamics with improved numerical dissipation: the generalized- α method”, *J. Appl. Mech. (ASME)* **60**:2 (1993), 371–375.
- [Dumouchel et al. 2007] P. E. Dumouchel, J.-J. Marigo, and M. Charlotte, “Rupture dynamique et fissuration quasi-statique instable”, *C. R. Mécanique* **335**:11 (2007), 708–713.
- [Francfort and Marigo 1998] G. A. Francfort and J.-J. Marigo, “Revisiting brittle fracture as an energy minimization problem”, *J. Mech. Phys. Solids* **46**:8 (1998), 1319–1342.
- [Francfort and Marigo 2002] G. A. Francfort and J.-J. Marigo, “Vers une théorie énergétique de la rupture fragile”, *C. R. Mécanique* **330**:4 (2002), 225–233.
- [Griffith 1921] A. Griffith, “The phenomena of rupture and flow in solids”, *Phil. Trans. R. Soc. A* **221**:582–593 (1921), 163–198.
- [Hentati 2013] H. Hentati, *Numerical method to simulate the dynamic crack propagation based on the variational approach*, thesis, University of Sfax, Tunisia, 2013.
- [Hentati et al. 2012a] H. Hentati, R. Abdelmoula, A. Maalej, and K. Maalej, “Quasi static analysis of anti-plane shear crack”, *Appl. Mech. Mater.* **232** (2012), 92–96.
- [Hentati et al. 2012b] H. Hentati, R. Abdelmoula, A. Maalej, and K. Maalej, “Quasi static fracture: global minimizer of the regularized energy”, *Appl. Mech. Mater.* **232** (2012), 97–101.
- [Hentati et al. 2013] H. Hentati, R. Abdelmoula, A. Maalej, and K. Maalej, “Numerical analysis solving the elastic dynamic problem”, *Int. J. Model. Identif. Control.* **19**:3 (2013), 299–305.
- [Hentati et al. 2015] H. Hentati, I. Ben Naceur, W. Bouzid, and A. Maalej, “Numerical analysis of damage thermo-mechanical models”, *Adv. Appl. Math. Mech.* **7**:5 (2015), 625–643.
- [Hofacker and Miehe 2012] M. Hofacker and C. Miehe, “Continuum phase field modeling of dynamic fracture: variational principles and staggered FE implementation”, *Int. J. Fract.* **178** (2012), 113–129.
- [Hofacker and Miehe 2013] M. Hofacker and C. Miehe, “A phase field model of dynamic fracture: robust field updates for the analysis of complex crack patterns”, *Int. J. Numer. Methods Eng.* **93**:3 (2013), 276–301.
- [Houbolt 1950] J. C. Houbolt, “A recurrence matrix solution for the dynamic response of elastic aircraft”, *J. Aeronaut. Sci.* **17** (1950), 540–550.
- [Jiang et al. 2012] C. P. Jiang, X. F. Wua, J. Li, F. Song, Y. F. Shao, X. H. Xu, and P. Yan, “A study of the mechanism of formation and numerical simulations of crack patterns in ceramics subjected to thermal shock”, *Acta Mater.* **60** (2012), 4540–4550.
- [Kalthoff 2000] J. F. Kalthoff, “Models of dynamic shear failure in solids”, *Int. J. Fract.* **101** (2000), 1–31.
- [Kim and Paulino 2004] J. H. Kim and G. H. Paulino, “Simulation of crack propagation in functionally graded materials under mixed-mode and non-proportional loading”, *Int. J. Mech. Mater. Des.* **1**:1 (2004), 63–94.
- [Miehe et al. 2010a] C. Miehe, M. Hofacker, and F. Welschinger, “A phase field model for rate-independent crack propagation: robust algorithmic implementation based on operator splits”, *Comput. Methods Appl. Mech. Eng.* **199**:45-48 (2010), 2765–2778.
- [Miehe et al. 2010b] C. Miehe, F. Welschinger, and M. Hofacker, “Thermodynamically consistent phase-field models of fracture: variational principles and multi-field FE implementations”, *Int. J. Numer. Methods Eng.* **83**:10 (2010), 1273–1311.
- [Msekh et al. 2015] M. A. Msekh, J. M. Sargado, M. Jamshidian, P. M. Areias, and T. Rabczuk, “Abaqus implementation of phase-field model for brittle fracture”, *Comput. Mater. Sci.* **96**:B (2015), 472–484.
- [Newmark 1959] N. M. Newmark, “A method of computation for structural dynamics”, *J. Eng. Mech. Div. (ASCE)* **85** (1959), 67–94.

- [Oleaga 2004] G. E. Oleaga, “On the path of a quasi-static crack in mode III”, *J. Elasticity* **76**:2 (2004), 163–189.
- [Pham and Marigo 2010a] K. Pham and J.-J. Marigo, “Approche variationnelle de l’endommagement, I: Les concepts fondamentaux”, *C. R. Mécanique* **338** (2010), 191–198.
- [Pham and Marigo 2010b] K. Pham and J.-J. Marigo, “Approche variationnelle de l’endommagement, II: Les modèles à gradient”, *C. R. Mécanique* **338** (2010), 199–206.
- [Schlüter et al. 2014] A. Schlüter, A. Willenbücher, C. Kuhn, and R. Müller, “Phase field approximation of dynamic brittle fracture”, *Comput. Mech.* **54**:5 (2014), 1141–1161.
- [Vignollet et al. 2014] J. Vignollet, S. May, R. de Borst, and C. V. Verhoosel, “Phase-field models for brittle and cohesive fracture”, *Meccanica (Milano)* **49**:11 (2014), 2587–2601.

Received 12 Jan 2016. Revised 27 Feb 2016. Accepted 3 Mar 2016.

HAMDI HENTATI: hamdi.hentati@yahoo.fr

LA2MP Laboratory, National School of Engineers of Sfax, University of Sfax, 3038 Sfax, Tunisia

MARWA DHAHRI: marwadhahri70@yahoo.com

LA2MP Laboratory, National School of Engineers of Sfax, University of Sfax, 3038 Sfax, Tunisia

FAKHREDDINE DAMMAK: fakhreddine.dammak@enis.rnu.tn

LA2MP Laboratory, National School of Engineers of Sfax, University of Sfax, 3038 Sfax, Tunisia

JOURNAL OF MECHANICS OF MATERIALS AND STRUCTURES

msp.org/jomms

Founded by Charles R. Steele and Marie-Louise Steele

EDITORIAL BOARD

ADAIR R. AGUIAR	University of São Paulo at São Carlos, Brazil
KATIA BERTOLDI	Harvard University, USA
DAVIDE BIGONI	University of Trento, Italy
YIBIN FU	Keele University, UK
IWONA JASIUK	University of Illinois at Urbana-Champaign, USA
C. W. LIM	City University of Hong Kong
THOMAS J. PENCE	Michigan State University, USA
GIANNI ROYER-CARFAGNI	Università degli studi di Parma, Italy
DAVID STEIGMANN	University of California at Berkeley, USA
PAUL STEINMANN	Friedrich-Alexander-Universität Erlangen-Nürnberg, Germany

ADVISORY BOARD

J. P. CARTER	University of Sydney, Australia
D. H. HODGES	Georgia Institute of Technology, USA
J. HUTCHINSON	Harvard University, USA
D. PAMPLONA	Universidade Católica do Rio de Janeiro, Brazil
M. B. RUBIN	Technion, Haifa, Israel

PRODUCTION production@msp.org

SILVIO LEVY Scientific Editor

See msp.org/jomms for submission guidelines.

JoMMS (ISSN 1559-3959) at Mathematical Sciences Publishers, 798 Evans Hall #6840, c/o University of California, Berkeley, CA 94720-3840, is published in 10 issues a year. The subscription price for 2016 is US \$575/year for the electronic version, and \$735/year (+\$60, if shipping outside the US) for print and electronic. Subscriptions, requests for back issues, and changes of address should be sent to MSP.

JoMMS peer-review and production is managed by EditFLOW[®] from Mathematical Sciences Publishers.

PUBLISHED BY

 **mathematical sciences publishers**
nonprofit scientific publishing

<http://msp.org/>

© 2016 Mathematical Sciences Publishers

- An Eulerian formulation for large deformations of elastically isotropic elastic-viscoplastic membranes** M. B. RUBIN and BEN NADLER 197
- Physical meaning of elastic constants in Cosserat, void, and microstretch elasticity** RODERIC S. LAKES 217
- On low-frequency vibrations of a composite string with contrast properties for energy scavenging fabric devices** ASKAR KUDAIBERGENOV, ANDREA NOBILI and LUDMILLA PRIKAZCHIKOVA 231
- Wave propagation in layered piezoelectric rings with rectangular cross sections** JIANGONG YU, XIAODONG YANG and JEAN-ETIENNE LEFEBVRE 245
- Effective boundary condition method and approximate secular equations of Rayleigh waves in orthotropic half-spaces coated by a thin layer** PHAM CHI VINH and VU THI NGOC ANH 259
- Nonlocal forced vibration of a double single-walled carbon nanotube system under the influence of an axial magnetic field** MARIJA B. STAMENKOVIĆ, DANILO KARLIČIĆ, GORAN JANEVSKI and PREDRAG KOZIĆ 279
- A phase-field model of quasistatic and dynamic brittle fracture using a staggered algorithm** HAMDİ HENTATI, MARWA DHAHRI and FAKHREDDINE DAMMAK 309